Electronic supplementary information (ESI)

Two Cu(I)-based inorganic-organic complexes assembled with polyoxometalate and thiacalix[4]arene for efficient catalytic reactions

Le Ma, Fei-Fan Guo* and Jian-Fang Ma*

Key Laboratory of Polyoxometalate and Reticular Material Chemistry of Ministry of Education, Department of chemistry, Northeast Normal Univetsity, Changchun, 130024, China

* Correspondence authors

E-mail: guoff527@nenu.edu.cn

E-mail: majf247@nenu.edu.cn

Experimental section

Materials and instrumentation. Chemicals are available commercially. Powder X-ray diffraction (PXRD) patterns were determined by using Rigaku Damx 2000 X-ray diffractometer with graphite monochromatized Cu Kα radiation (λ = 0.154 Å). IR spectra were recorded with a Nicolet Magna 560 Fourier transform IR spectrometer. ICP measurements were conducted on a Leeman Laboratories Prodigy inductively coupled plasma-optical atomic emission spectrometer (ICP-AES). C, H and N contents were carried out on a Euro vector EA3000 elemental analyzer. ^{1}H NMR data were recorded in $CDCl_3$ on a Bruker 500 MHz. X-ray photoelectron spectroscopy (XPS) was determined with an Escalab 250 instrument. Energy dispersive x-ray spectroscopy (EDS) was obtained by GeminiSEM 300 and AZtecLive UltimMax100. TGA data was recorded on a DTG-60H under N_2 atmosphere. Products of AAC reactions were detected by GC equipment with capillary (30 m long×0.25 mm i.d., WondaCAP 17), and FID detector (GC-2014C, Shimadzu, Japan). Yields of catalytic reactions were measured with high performance liquid chromatography (HPLC) and gas chromatography (GC). ODS products were detected by HPLC with a UV-vis detector at λ = 254 nm using an Inertsil (5 μm, 4.6×150 mm) ODS C18 column (Agilent-1220).

X-ray crystallography. Crystallographic data were measured on an Oxford Diffraction Gemini R CCD diffractometer with graphite monochromated Mo Kα radiation (λ = 0.71073 Å). Structures were solved by direct methods with SHELXT-2018/3[1] and refined on F^2 by full-matrix least-squares with SHELXTL-2018/3 within WINGX.[2-3] Non-hydrogen atom was refined anisotropically. Carbon hydrogen atoms were placed geometrically. SQUEEZE routine was applied to remove the disordered solvents. Crystallographic data of **1** and **2** are presented in Table S1. Selected bond distances and angles were provided in Table S2.

Synthesis of L$_1$. Thiacalix[4]arene precursors were synthesized according to the literature method (Scheme S1).[4,5] A mixture of K_2CO_3 (5.745 g, 50 mmol) and 2-mercaptopyrimidine (2.8 g, 25 mmol) were dissolved in dry DMF (200 mL). The

precursor B (2.805 g, 25 mmol) was added to the mixture in water bath under N_2 for 12 h. After the reaction finished, the mixture was sealed in a single-necked bottle. Then the mixture was cooled and the solvent was removed. L_1 ligand was obtained by filtration and washed with water for several times (yield: 79%). ^{1}H NMR (500 MHz, CDCl$_3$): δ 8.54 (dd, 8H), 7.51 (s, 8H), 6.98 (m, 4H), 4.26 (m, 8H), 2.84 (m, 8H), 1.12 (s, 36H). IR (KBr, cm^{-1}): 3029 (w), 2955 (m), 2864 (m), 1551 (s), 1463 (w), 1434 (m), 1372 (s), 1262 (s), 1180 (s), 1079 (m), 988 (s), 882 (m), 830 (w), 800 (m), 746 (s), 706 (w), 626 (w), 591 (w), 541 (w), 475 (w), 442 (w).
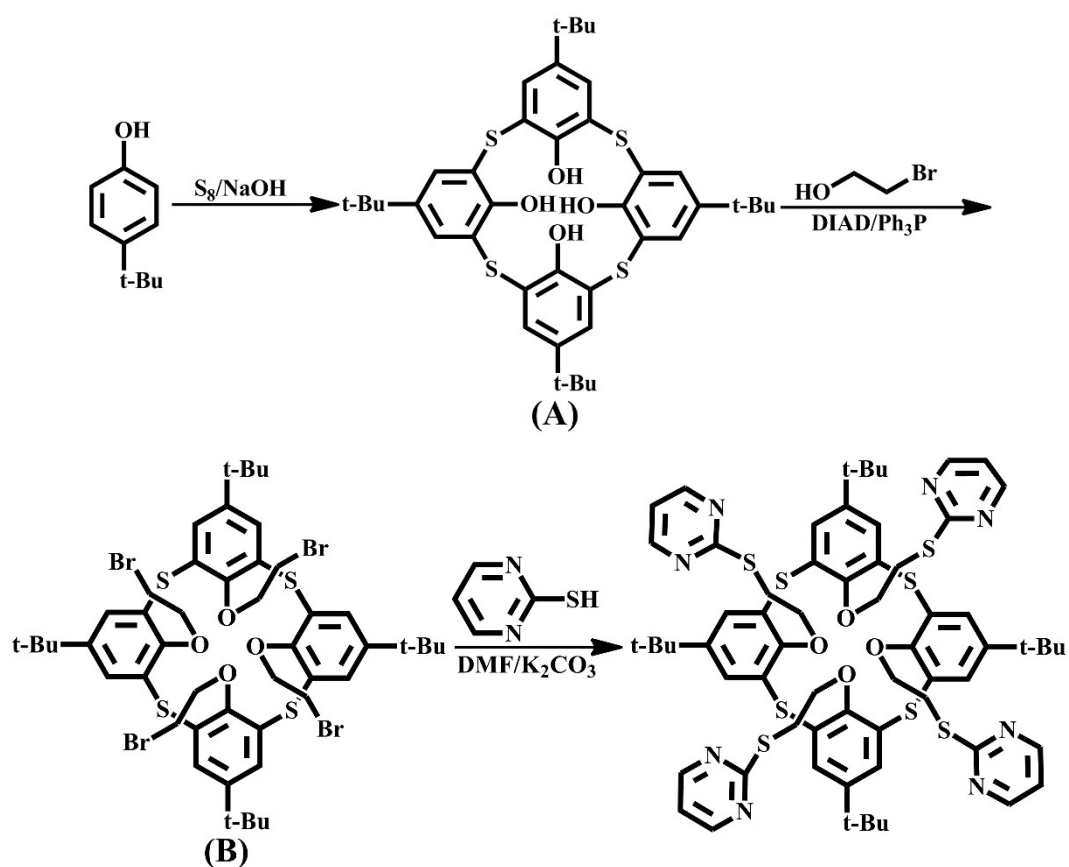
Scheme S1. Synthetic route of L_1 ligand.

Preparation of [H$_3$O]·[CuL]·0.5[Mo$_{10}$O$_{32}$]·H$_2$O (1). A mixture of CuCl$_2$·2H$_2$O (8 mg, 0.04 mmol), L_1 (13 mg, 0.01 mmol), [(n-C$_4$H$_9$)$_4$N]$_4$[Mo$_8$O$_{26}$] (28 mg, 0.012 mmol), ethanol (4 mL) and methanol (4 mL) were sealed in a Teflon reactor (15 mL) and heated at 120 °C for 3 days. After cooling to room temperature, deep bule crystals were achieved in 26% yield. Anal. Calcd (%) for C$_{56}$H$_{73}$CuN$_4$O$_{24}$S$_6$Mo$_5$ (*Mr* = 1921.83): C, 35.00; H, 3.83; N, 2.92. Found: C, 34.76; H, 3.68; N, 3.04. IR data (KBr, cm^{-1}): 2955

(m), 2867 (w), 1659 (w), 1549 (m), 1463 (w), 1431 (w), 1374 (s), 1262 (w), 1234 (w), 1182 (m), 1081 (w), 988 (m), 951 (s), 882 (m), 747 (s), 677 (m), 628 (m), 580 (m), 541 (s), 434 (s).

Preparation of [CuL]·0.5[HPW$_{12}$O$_{40}$]·EtOH·H$_2$O (2). 2 was prepared with a similar method to that of **1** except that [(n-C$_4$H$_9$)$_4$N]$_4$[Mo$_8$O$_{26}$] (28 mg, 0.012 mmol) and CuCl$_2$·2H$_2$O (8 mg, 0.04 mmol) were replaced by H$_3$PW$_{12}$O$_{40}$ (29 mg, 0.01 mmol) and CuBr$_2$ (9 mg, 0.04 mmol), respectively, and heated at 130 °C in a mixed solution of ethanol (6 mL) and deionized water (2 mL) for 72 h. The yellow flake crystals were obtained in 78% yield. Anal. Calcd (%) for C$_{58}$H$_{76.5}$CuN$_4$O$_{28}$S$_6$P$_{0.5}$W$_6$ (Mr = 2652.21): C, 26.27; H, 2.91; N, 2.11. Found: C, 25.98; H, 2.83; N, 2.19. IR data (KBr, cm^{-1}): 3745 (w), 2955 (w), 2865 (w), 1648 (w), 1547 (m), 1463 (w), 1430 (w), 1380 (m), 1262 (m), 1234 (w), 1186 (m), 1076 (m), 975 (s), 891 (m), 794 (s), 751 (s), 591 (m), 513 (s).

Catalytic ODS reaction of 1. Biphenyl (0.4 mmol), CH$_2$Cl$_2$ (5 mL), TBHP (1 mmol), catalyst **1** (10 mg) and substrate (0.4 mmol) were placed in a 38 mL pressure-proof pipe. The resulting mixture was stirred at 25 °C. GC or HPLC was used to record the conversion rate (Fig. S4-S8). When catalyst **1** was replaced by [(n-C$_4$H$_9$)$_4$N]$_4$[Mo$_8$O$_{26}$], CuCl$_2$·2H$_2$O and L, the corresponding catalyst doses were 7 mg, 0.9 mg and 6.5 mg, respectively.

Catalytic AAC reaction of 2. Alkynes (2 mmol), amyl acetate (0.92 mmol), methanol (4mL), azides (1 mmol) and **2** (10 mg) were placed in a 38 mL pressure-proof pipe at 70 °C for 8 h. The conversion rate was measured with GC or HPLC. Catalytic product was further characterized with ^{1}H NMR (Fig. S10-S14). When catalyst **1** was replaced by L, the L dose was 4.7 mg.
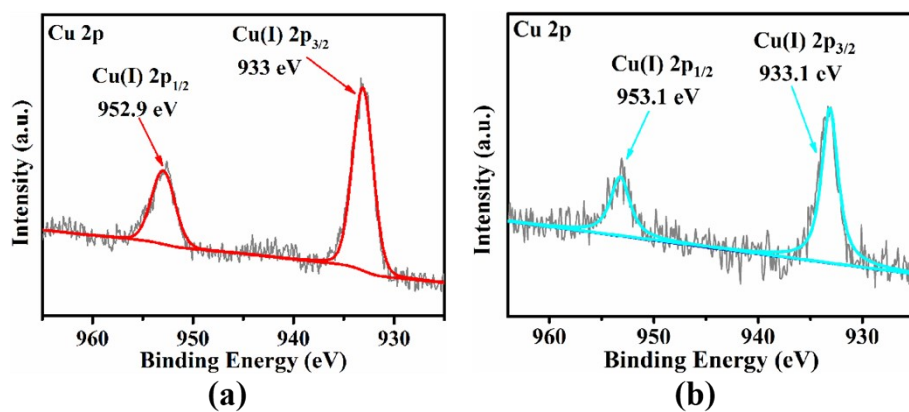
Fig. S1 XPS spectra of Cu 2p in (a) **1** and (b) **2**.
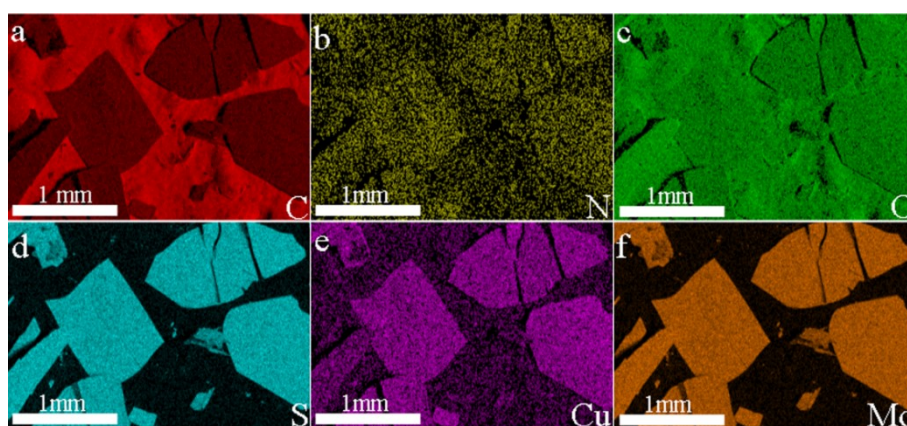
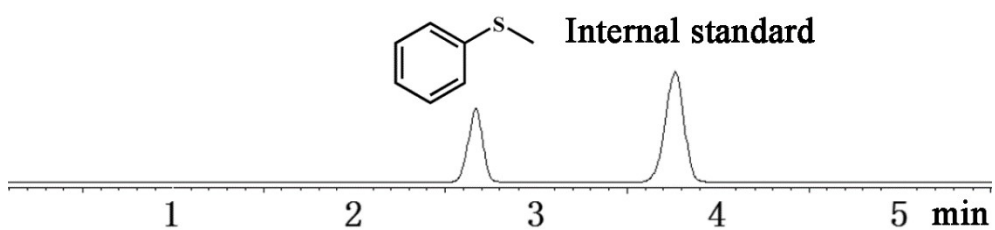**Fig. S2** EDS elemental mapping images of **1.**
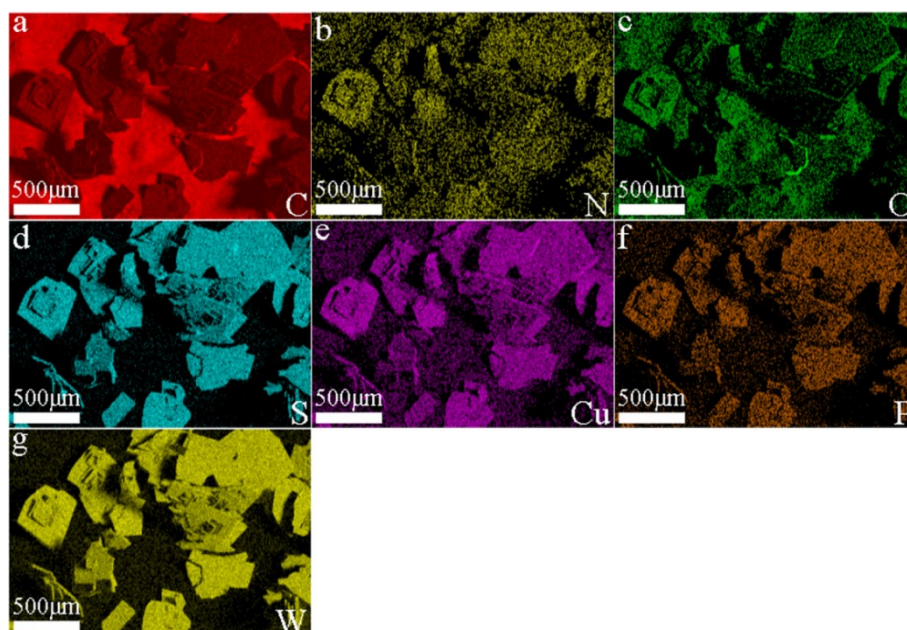
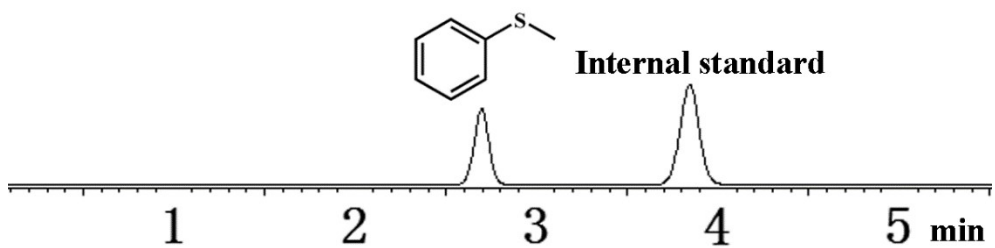**Fig. S3** EDS elemental mapping images of **2.**
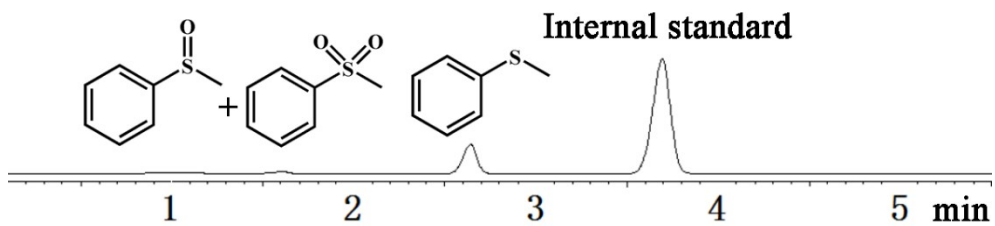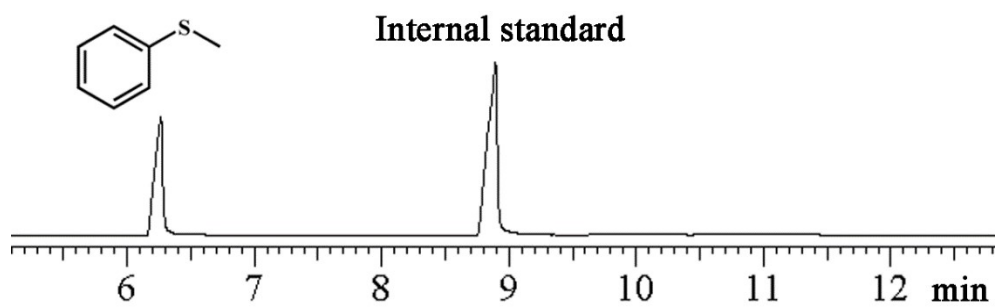
(a)
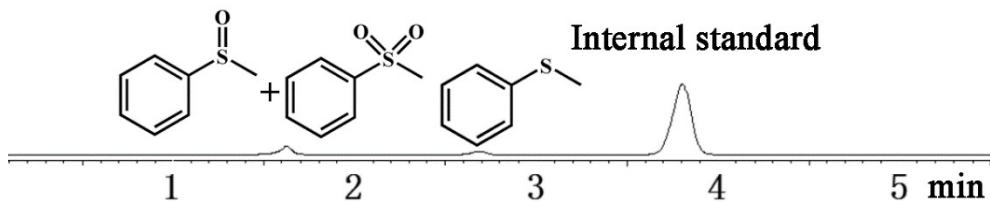
(b)
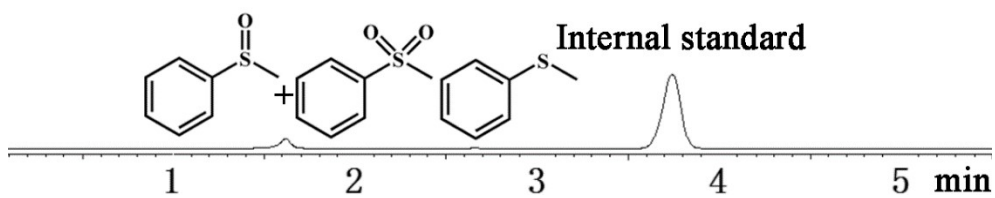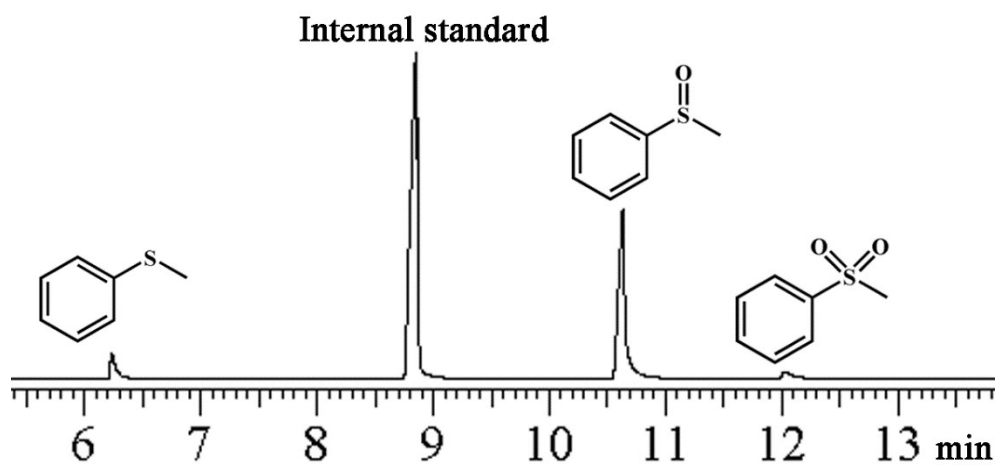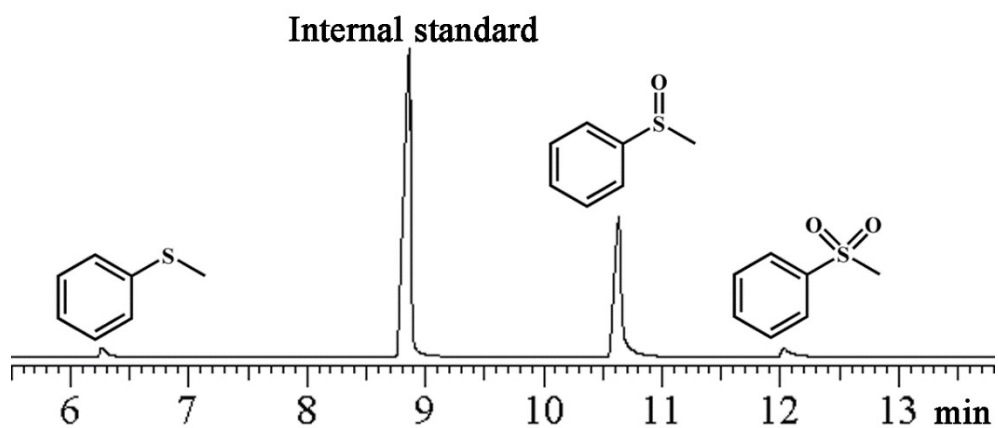

(c)
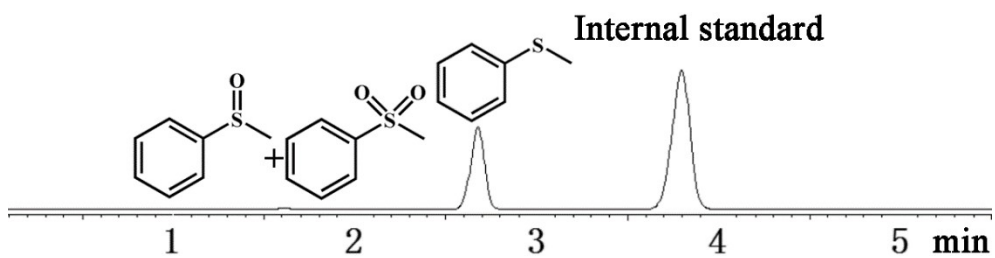
(d)

(e)

(f)

Fig. S4 HPLC of ODS for MBT with TBHP as oxidant in CH_2Cl_2 at 25 °C. (a) **1** as catalyst for 1 h, (b) **1** as catalyst for 2 h, (c) **1** as catalyst for 3 h, (d) $[(n\text{-}C_4H_9)_4N]_4[Mo_8O_{26}]$ as catalyst for 3 h, (e) $CuCl_2 \cdot 2H_2O$ as catalyst for 3 h, (f) L as catalyst for 3 h.

(a)

(b)

(c)
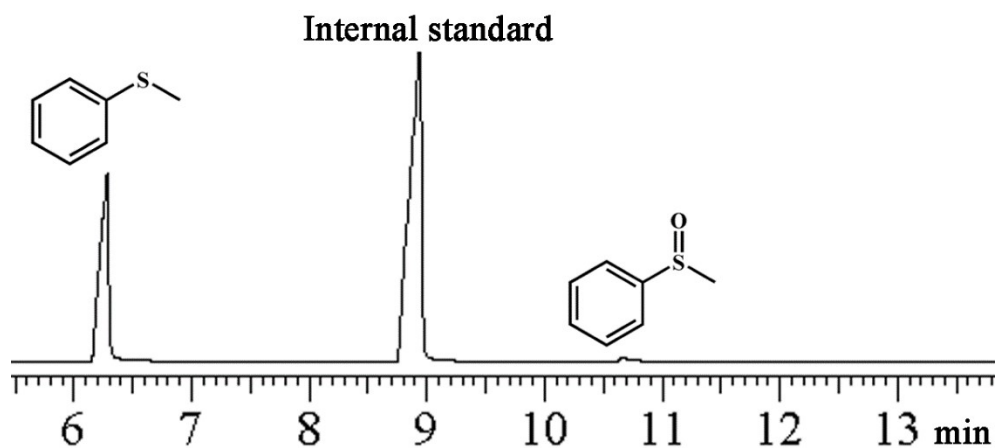
(d)

Fig. S5 GC of ODS for MBT in CH$_2$Cl$_2$ at 25 °C. (a) **1** as catalyst and H$_2$O$_2$ as oxidant for 3 h, (b) MBT as the substrate, **1** as catalyst and TBHP as oxidant in methanol at 25 °C for 3 h, (c) MBT as the substrate, **1** as catalyst and TBHP as oxidant in ethanol at 25 °C for 3 h and (d) TBHP as oxidant for 3 h.
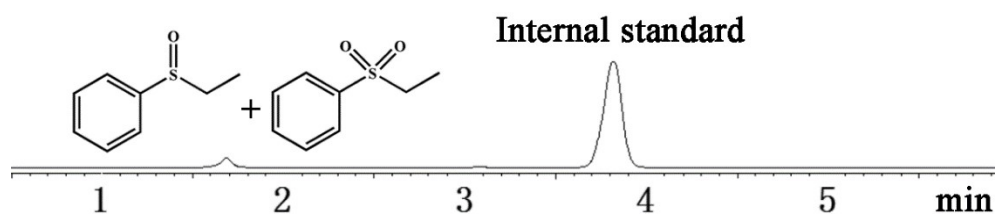
(a)
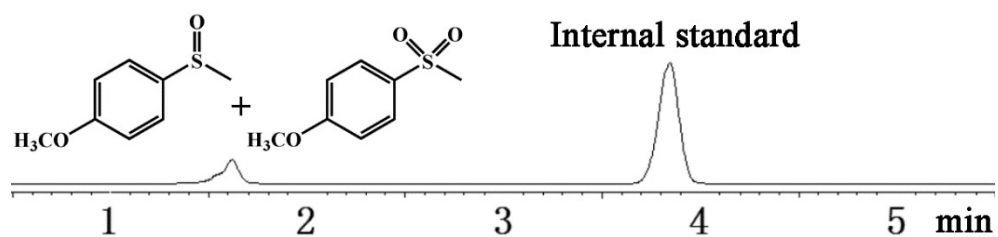
(b)
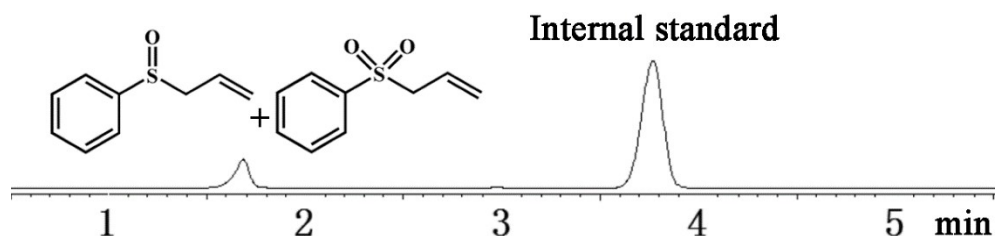
(c)
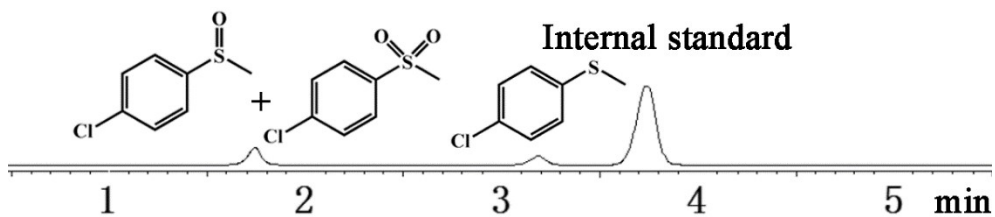
(d)
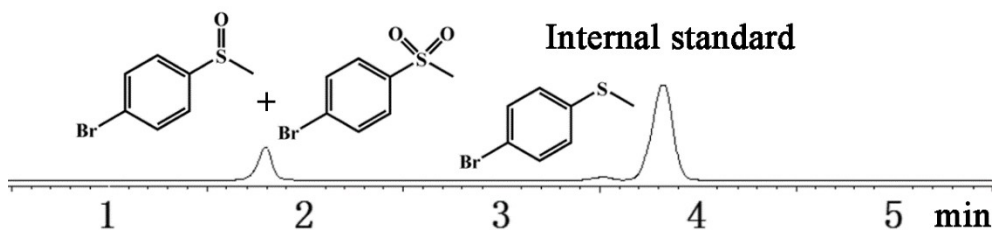
(e)
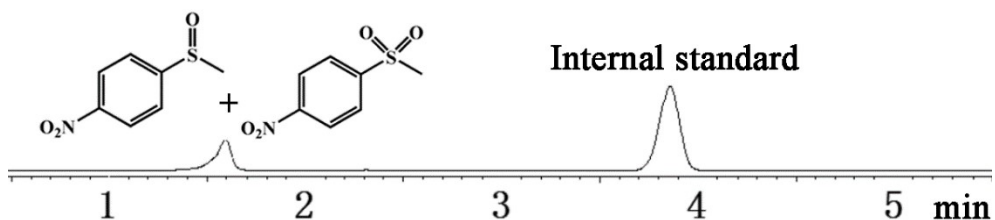
(f)
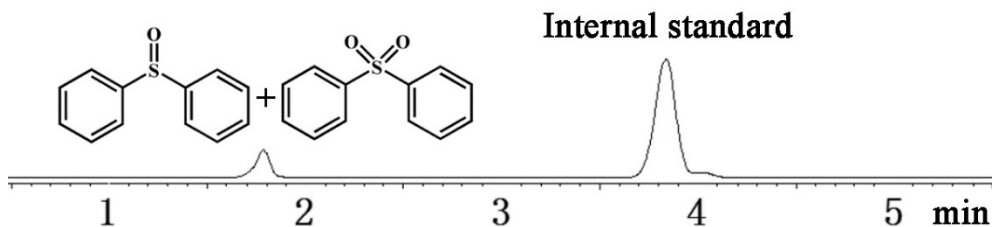
(g)
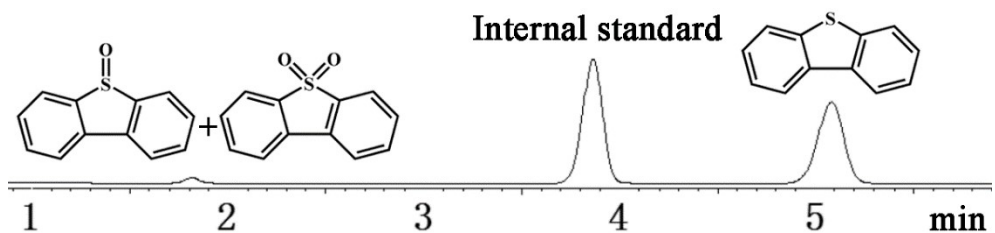
(h)
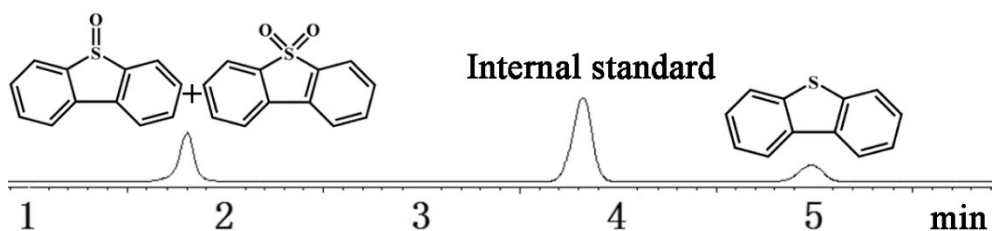
(i)
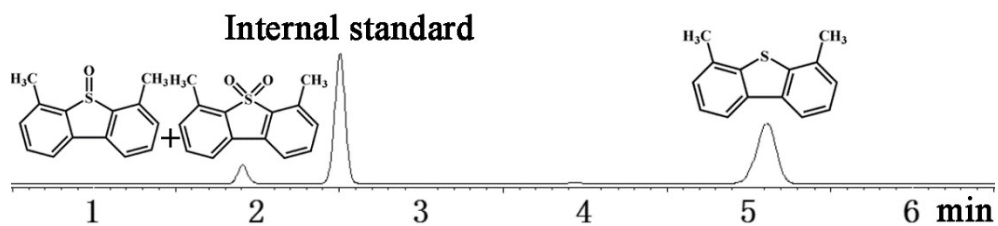
(j)
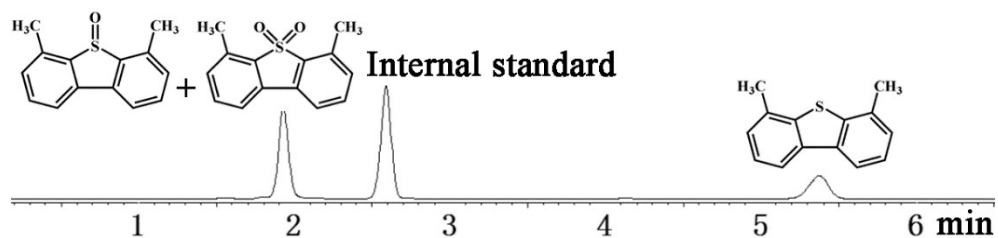
(k)
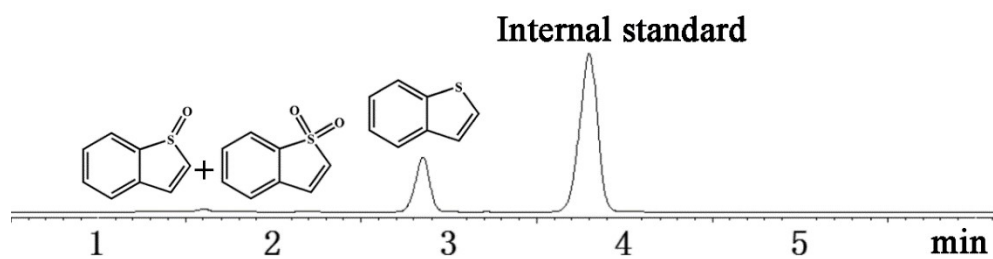
(l)

Fig. S6 HPLC of ODS for different sulfide substrates with TBHP as oxidant and **1** as catalyst in CH$_2$Cl$_2$ at 25 °C. (a) With ethylphenylsulfide for 3 h, (b) with 4-methoxythioanisole for 3 h, (c) with allylphenylsulfide for 3 h, (d) with 4-chlorothioanisole for 3 h, (e) with 4-bromothioanisole for 3 h, (f) with 4-nitrothioanisole for 3 h, (g) with diphenylsulfide for 3 h, (h) with dibenzothiophene for 3 h, (i) with dibenzothiophene for 12 h, (j) with 4,6-dimethyldibenzothiophene for 3 h, (k) with 4,6-dimethyldibenzothiophene for 12 h and (l) with benzothiophene for 12 h.
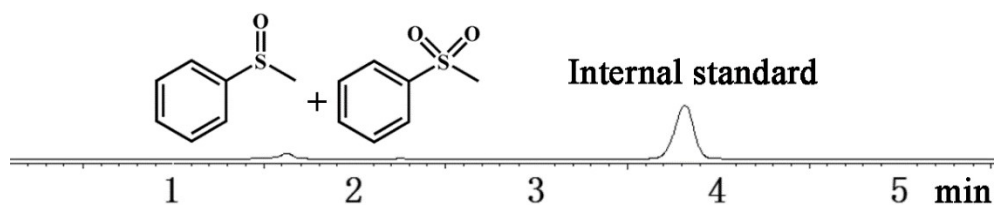

(a)

10
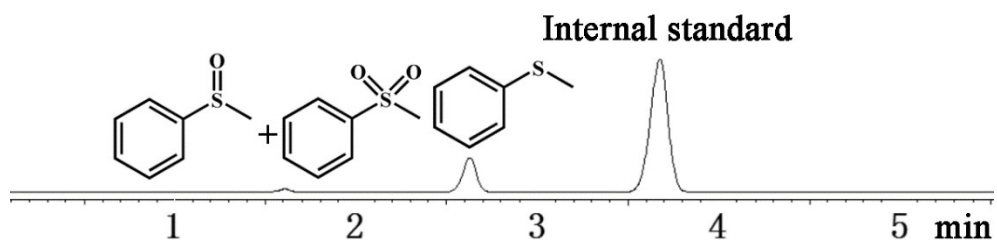
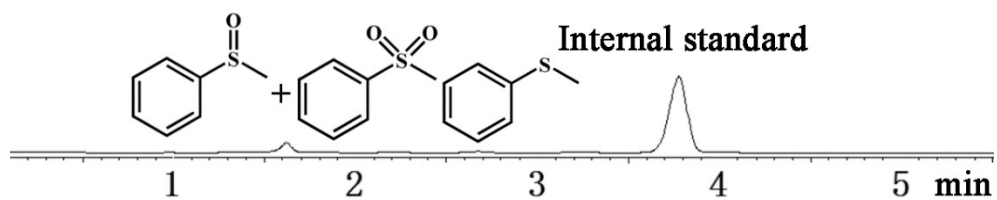**(b)**
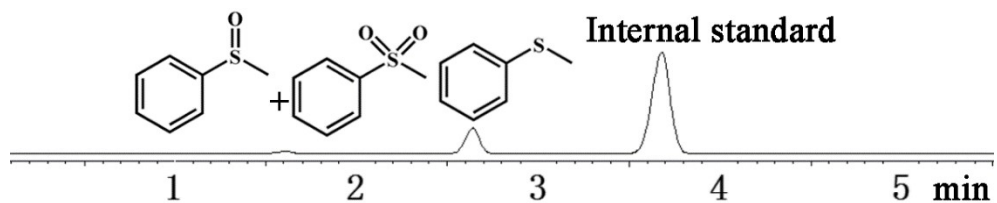
(c)

Fig. S7 HPLC of ODS for MBT with TBHP as oxidant in CH$_2$Cl$_2$ at 25 °C. (a) With **1** for 1 h, (b) the filtrate for 1 h after removing **1** of the catalytic reaction for 1 h and (c) the filtrate for 2 h after removing **1** of the catalytic reaction for 1 h.
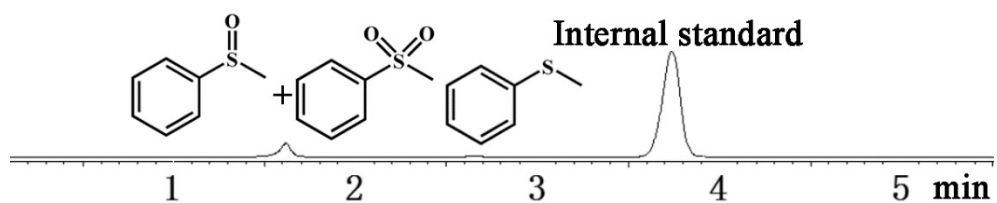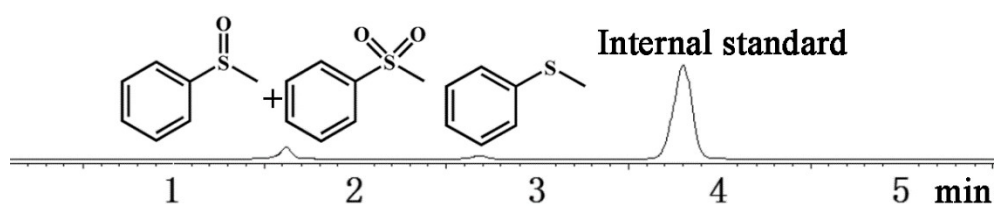

(a)

(b)

(c)

(d)

Fig. S8 HPLC of ODS for MBT with **1** as catalyst in different circles. (a) The first circle, (b) the second circle, (c) the third circle and (d) the fourth circle.
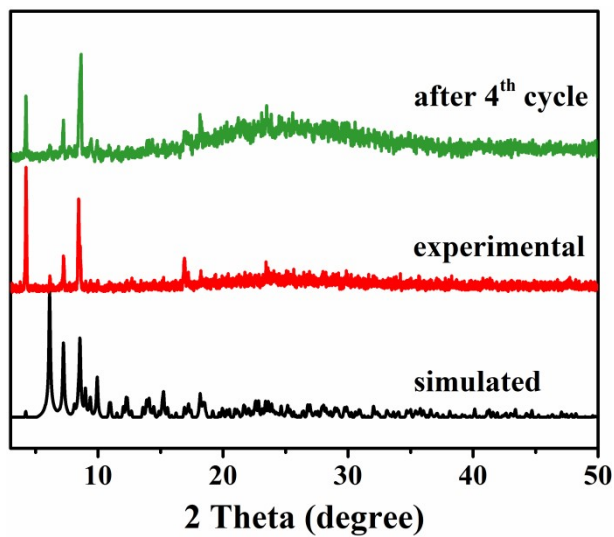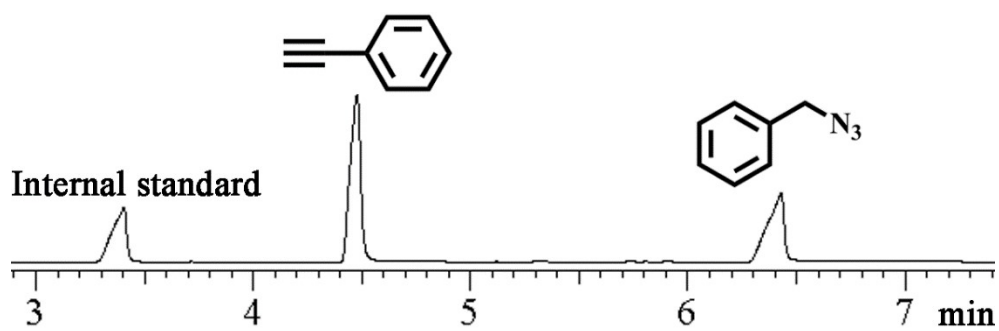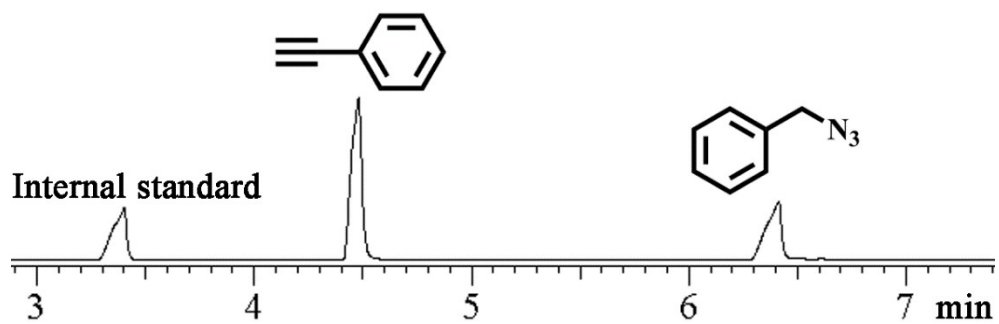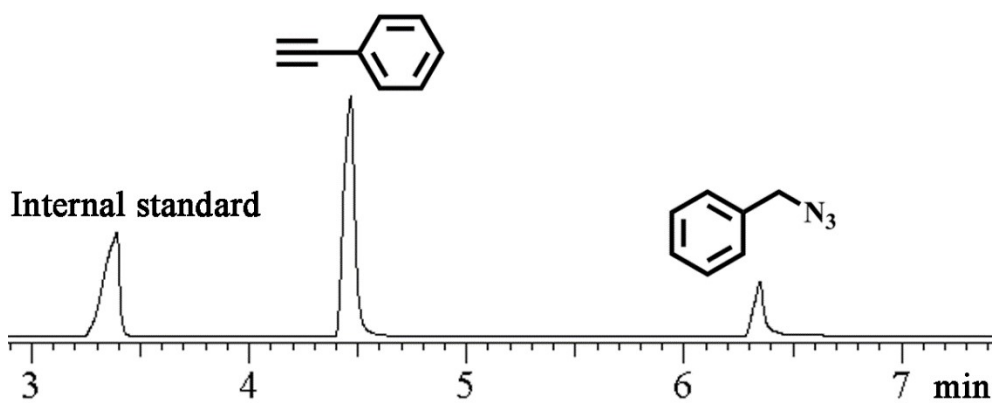

Fig. S9 PXRD patterns for the experimental **1**, the simulated **1** and the recycled **1**.

(a)

(b)

(c)

(d)

(e)

(f)

13
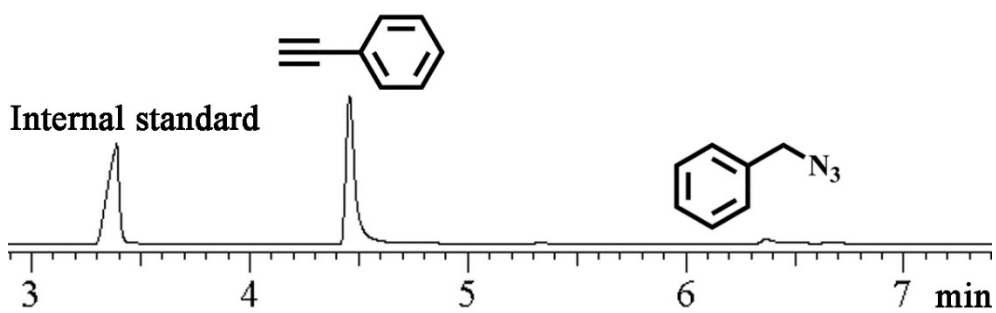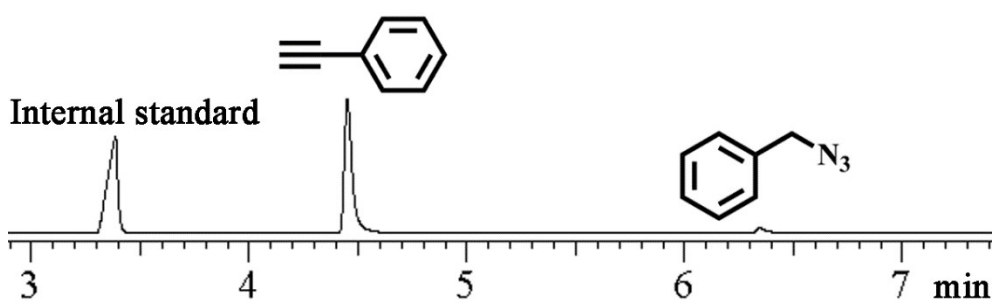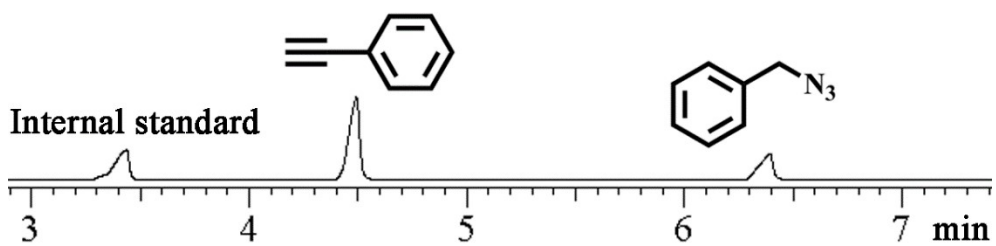
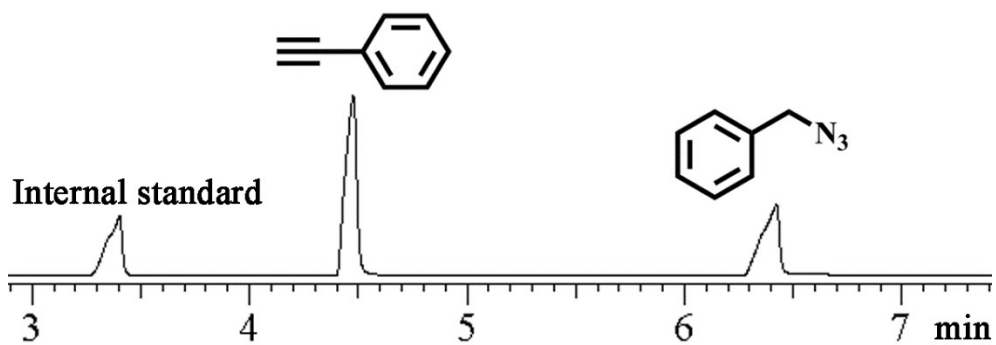**(g)**
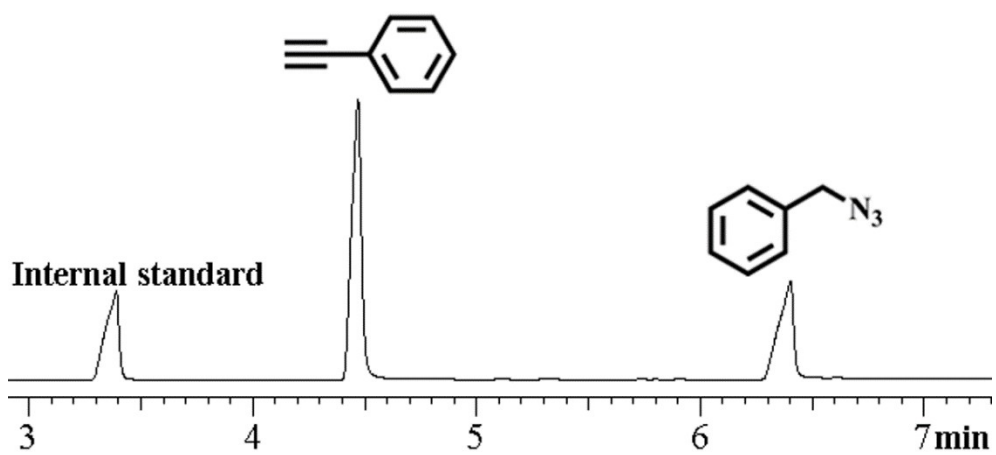
(h)
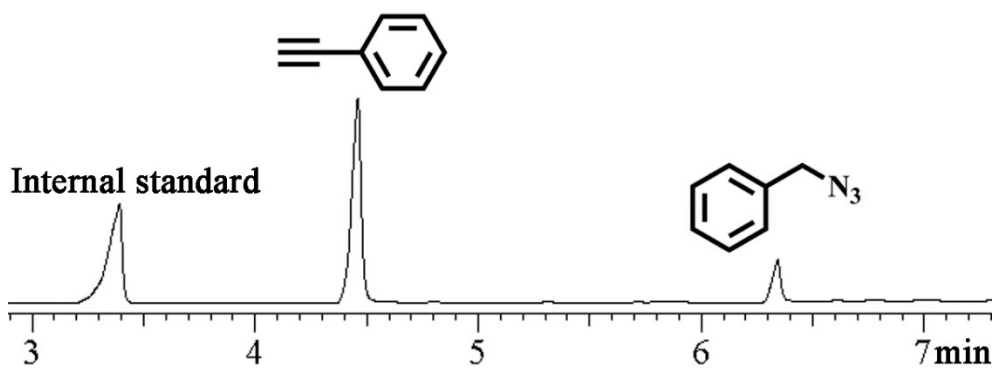
(i)
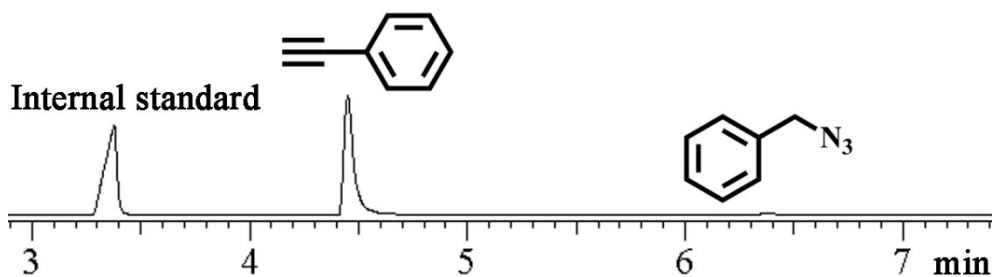
(j)

Fig. S10 GC of AAC reaction between the benzyl azide and phenylacetylene under

14

various conditions. (a) With **2** (10 mg) in CH$_3$OH at 25 °C for 8 h, (b) with **2** (10 mg) in CH$_3$OH at 40 °C for 8 h, (c) with **2** (10 mg) in CH$_3$OH at 60 °C for 8 h, (d) with **2** (10 mg) in CH$_3$OH at 70 °C for 8 h, (e) with **2** (10 mg) in CH$_3$CH$_2$OH at 70 °C for 8 h, (f) with **2** (10 m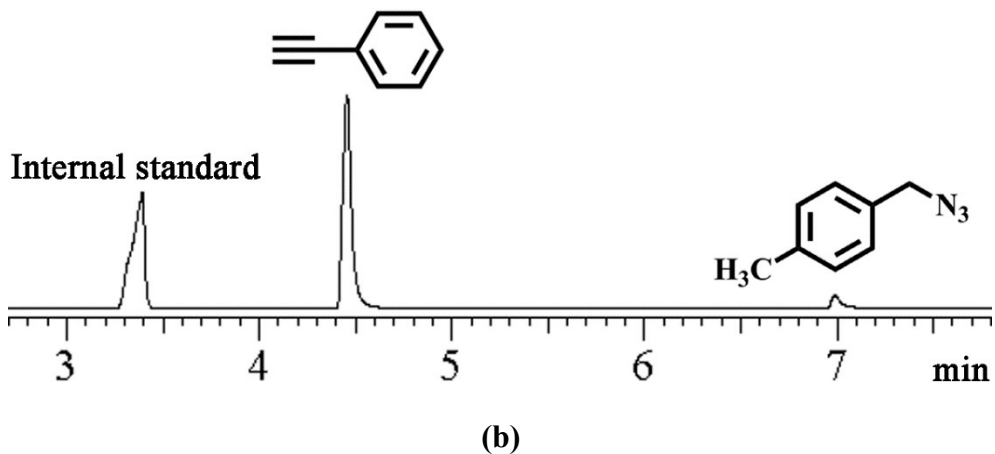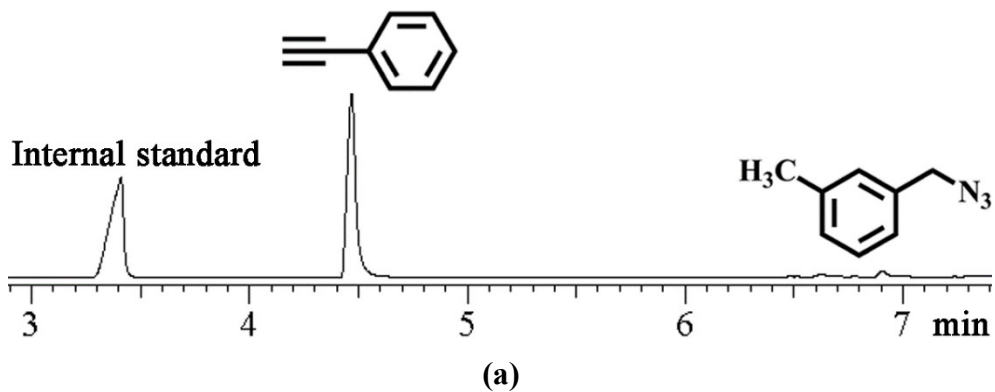g) in CH$_3$CN at 70 °C for 8 h, (g) with **2** (0 mg) in CH$_3$OH at 70 °C for 8 h, (h) with L (4.7 mg) in CH$_3$OH at 70 °C for 8 h, (i) with **2** (5 mg) in CH$_3$OH at 70 °C for 8 h and (j) with **2** (15 mg) in CH$_3$OH at 70 °C for 8 h.

(a)

(b)

(c)

15
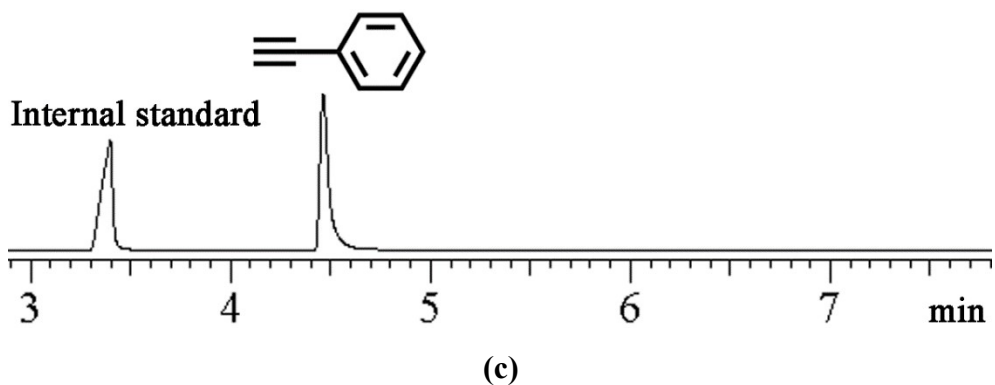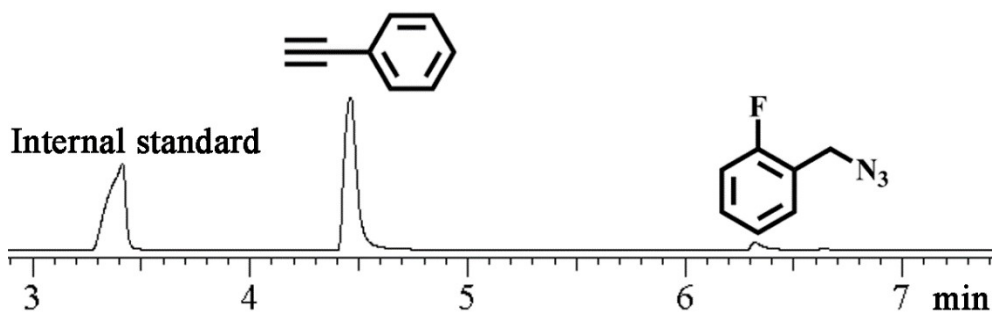
(d)
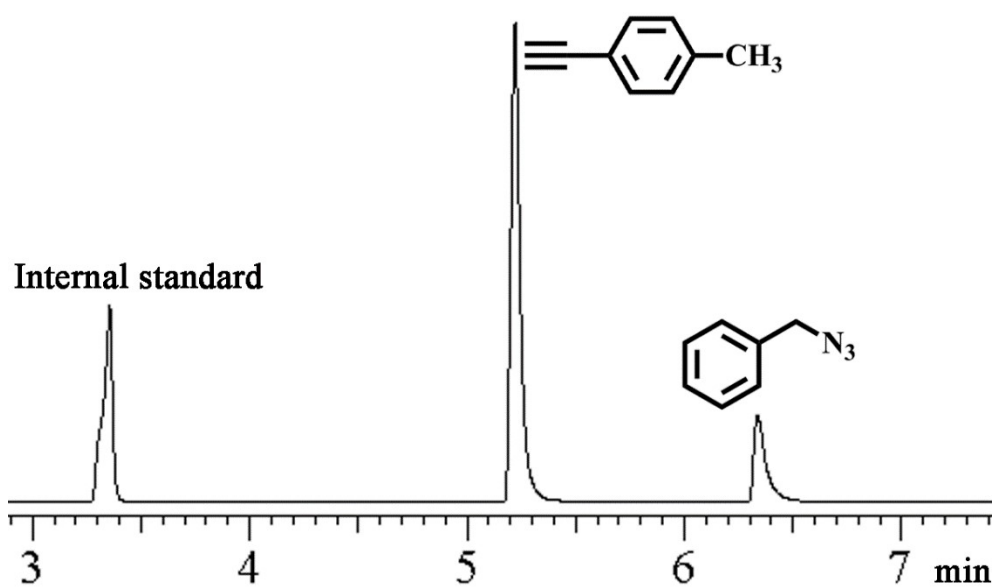
(e)

(f)

(g)

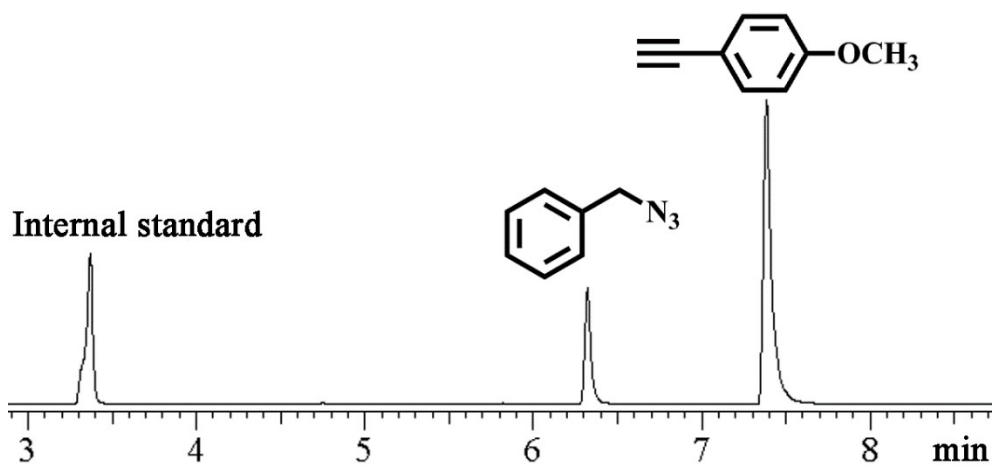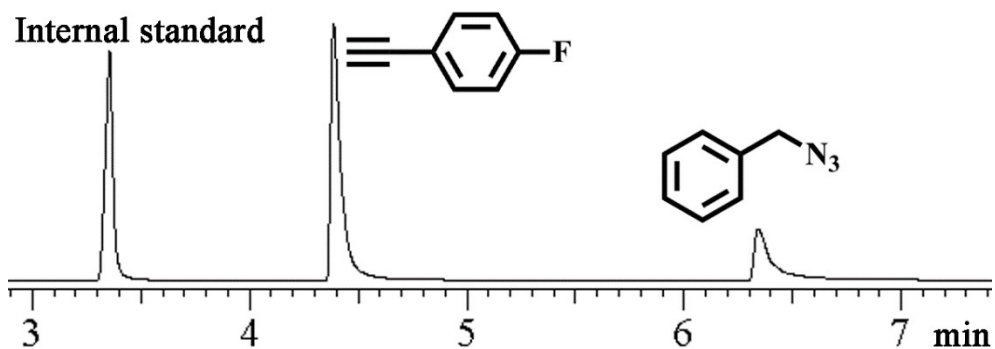**Fig. S11** GC of AAC reactions for the substituted benzyl azides and phenylacetylenes with different groups under the same condition (with 10 mg of **2** in CH₃OH at 70 °C for 8 h). (a) With 1-(azidomethyl)-3-methylbenzene and phenylacetylene as substrates, (b) 1-(azidomethyl)-4-methyl-benzene and phenylacetylene as substrates, (c) 1-(azidomethyl)-4-nitrobenzene and phenylacetylene as substrates, (d) 1-(azidomethyl)-2-fluorobenzene and phenylacetylene as substrates, (e) benzyl azide and 4-methylphenylacetylene as substrates, (f) benzyl azide and 4-methoxyphenylacetylene as substrates and (g) benzyl azide and 4-fluorophenylacetylene as substrates.

(a)

17
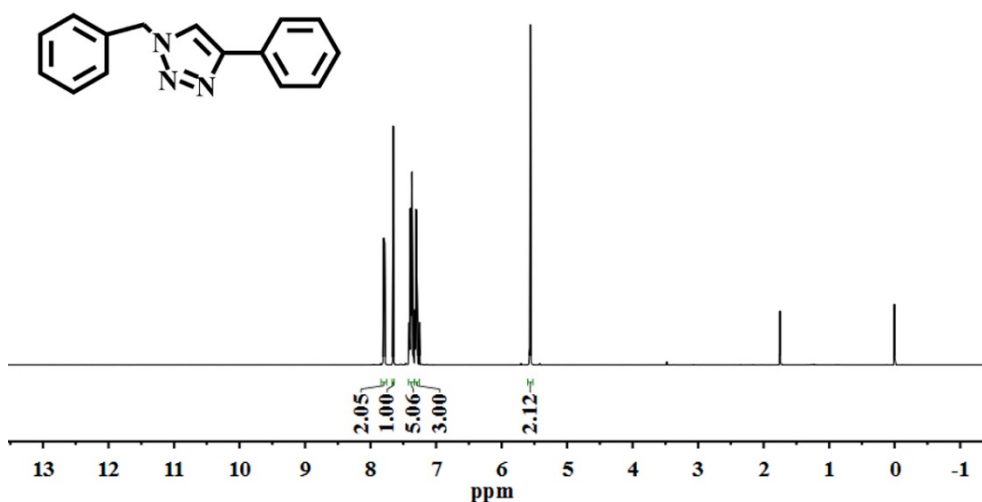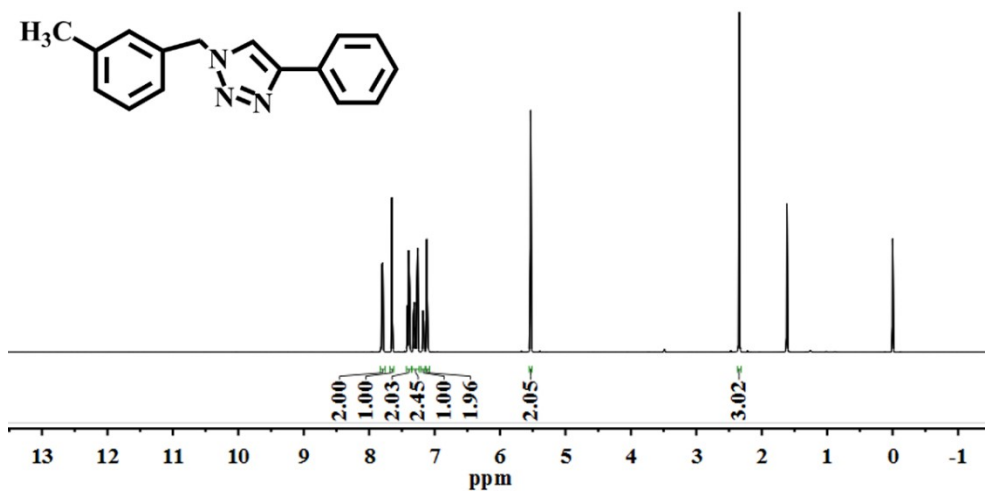
(b)
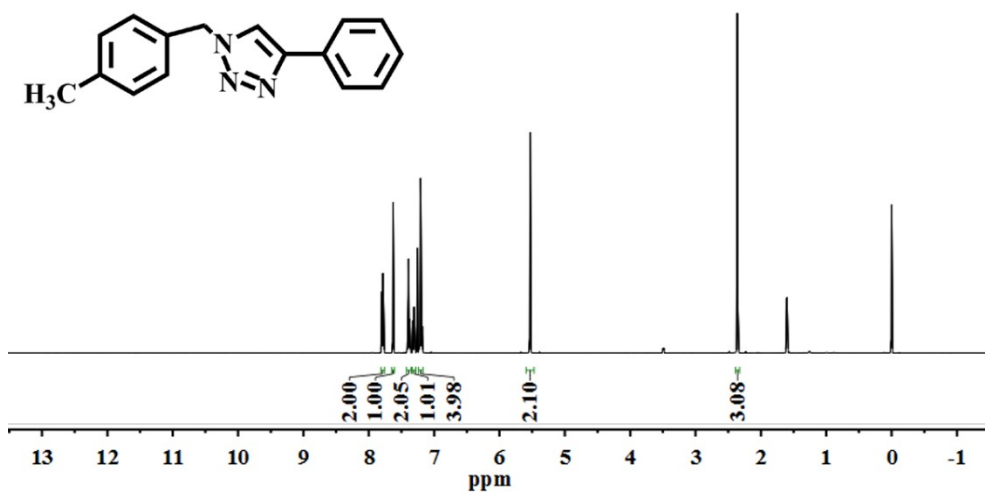
(c)
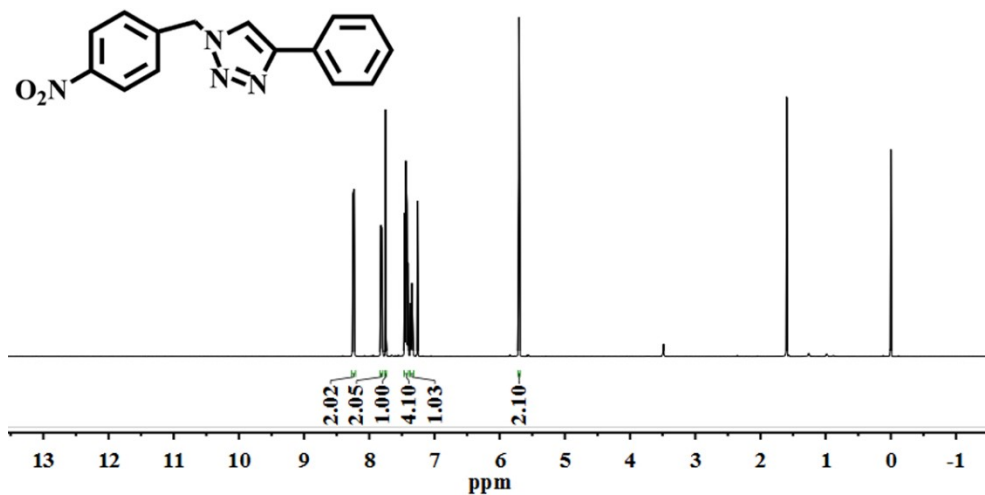
(d)
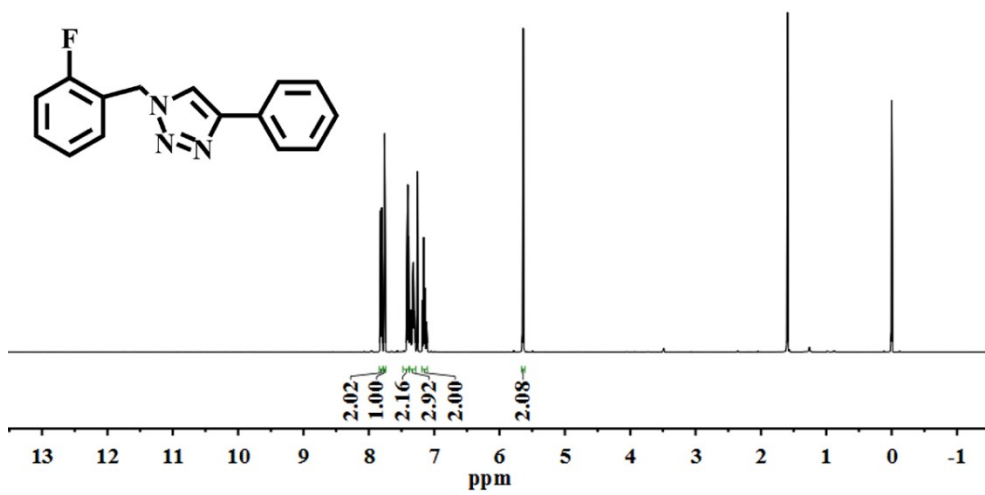
(e)
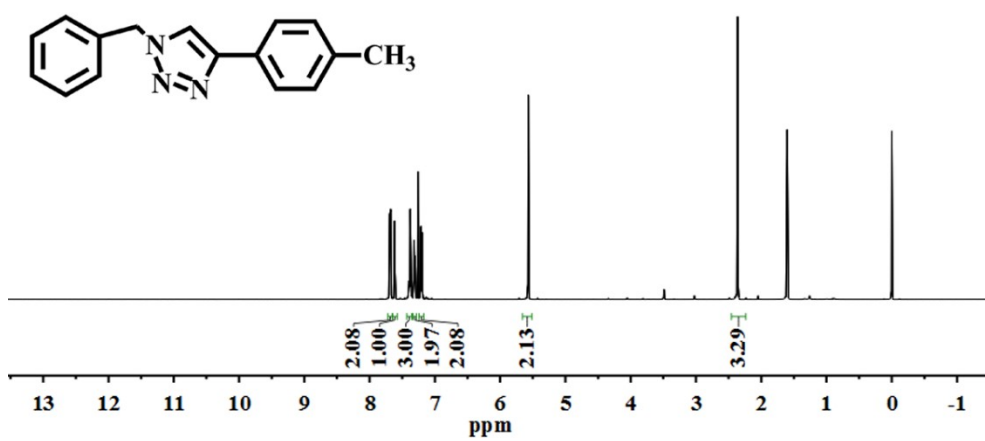
(f)
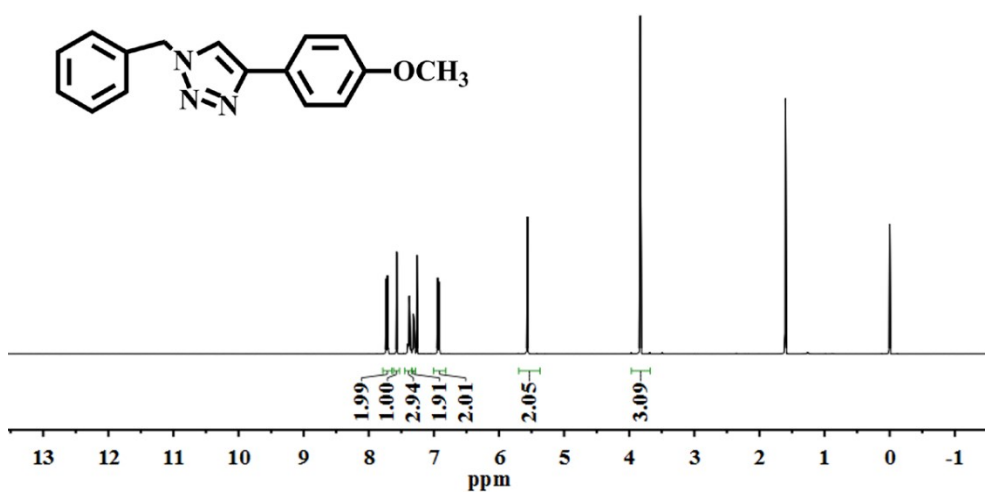
(g)
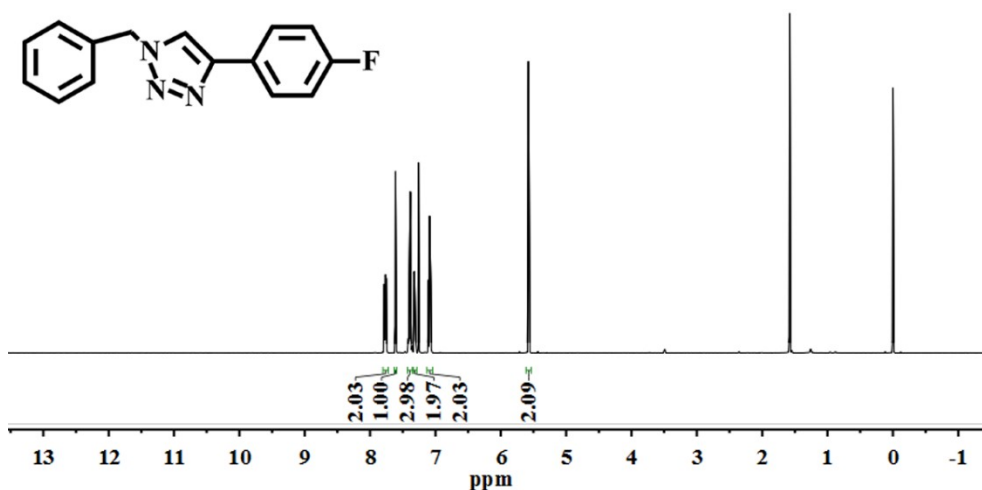
(h)

Fig. S12 ^{1}H NMR (500 MHz, CDCl$_3$). (a) With 1-benzyl-4-phenyl-1H-1,2,3-triazole, (b) 1-(3-methylbenzyl)-4-phenyl-1H-1,2,3-triazole, (c) 1-(4-methylbenzyl)-4-phenyl-1H-1,2,3-triazole, (d) 1-(4-nitrobenzyl)-4-phenyl-1H-1,2,3-triazole, (e) 1-(2-fluorobenzyl)-4-phenyl-1H-1,2,3-triazole, (f) 1-benzyl-4-(4-methyl-phenyl)-1H-1,2,3-triazole, (g) 1-benzyl-4-(4-methoxy-phenyl)-1H-1,2,3-triazole and (h) 1-benzyl-4-(4-fluoro-phenyl)-1H-1,2,3-triazole.

(a)

(b)
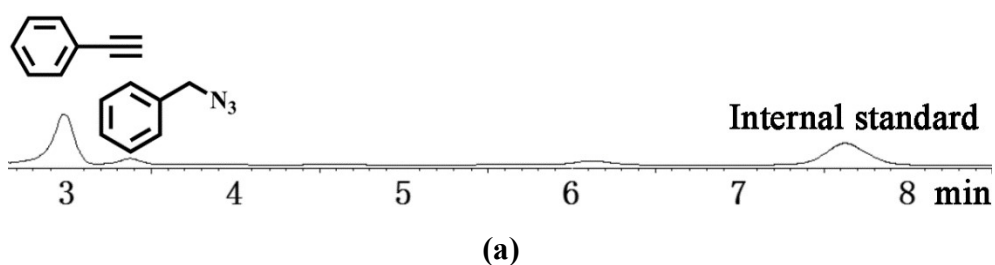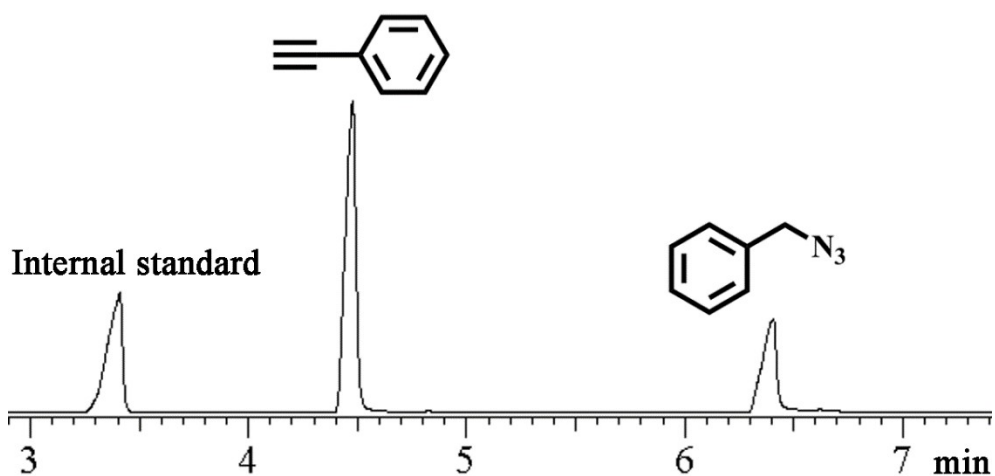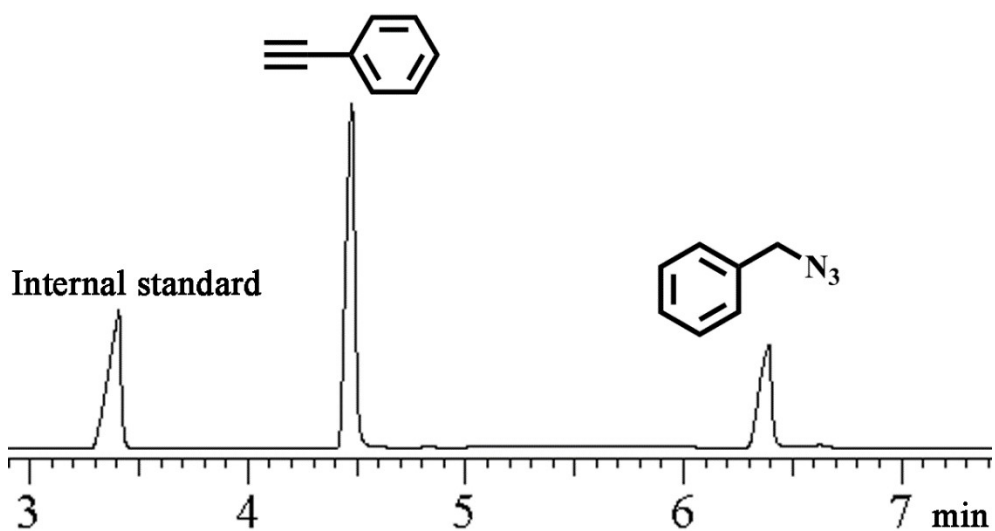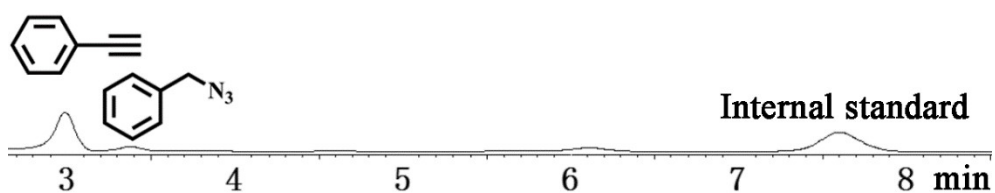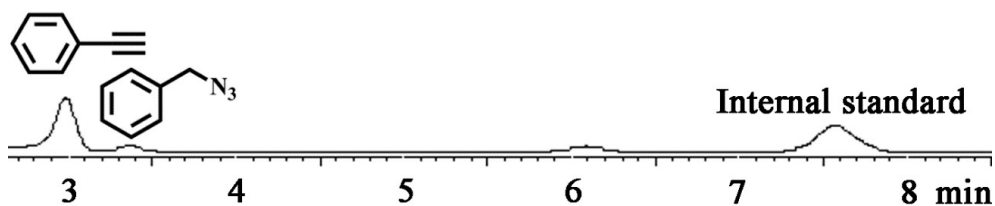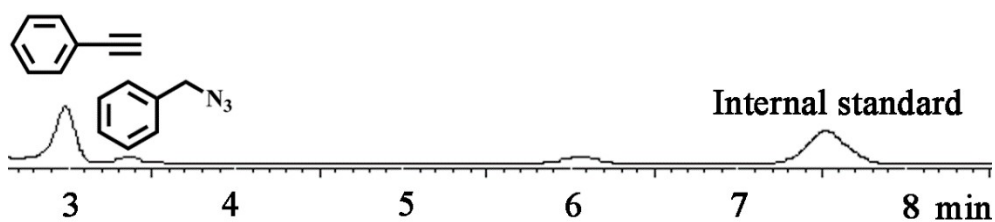
Fig. S13 HPLC and GC of AAC reactions for benzyl azide and phenylacetylene with kinetic and hot filtration experiments. (a) With **2** (10 mg) in CH$_3$OH at 70 °C for 2 h, (b) with **2** (10 mg) in CH$_3$OH at 70 °C for 4 h, (c) with **2** (10 mg) in CH$_3$OH at 70 °C for 6 h, (d) the filtrate in CH$_3$OH for 4 h after removing **2** of the catalytic reaction for 2 h, (e) the filtrate in CH$_3$OH for 6 h after removing **2** of the catalytic reaction for 2 h and (f) the filtrate in CH$_3$OH for 8 h after removing **2** of the catalytic reaction for 2 h.
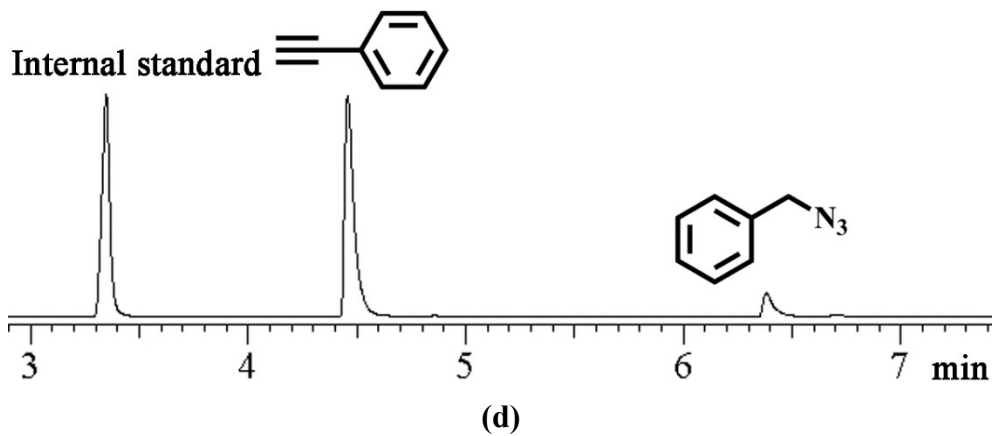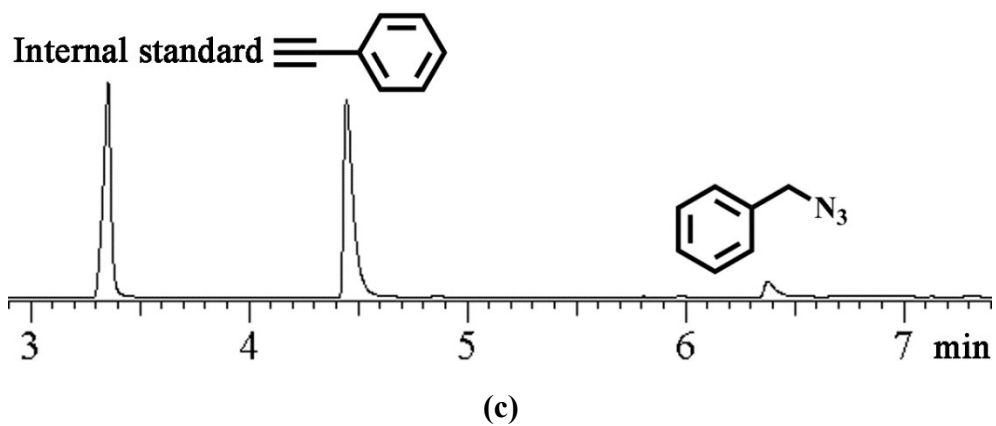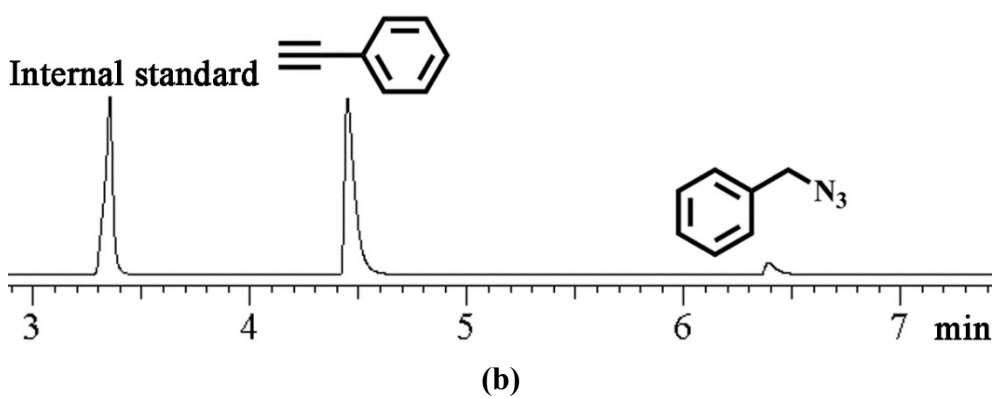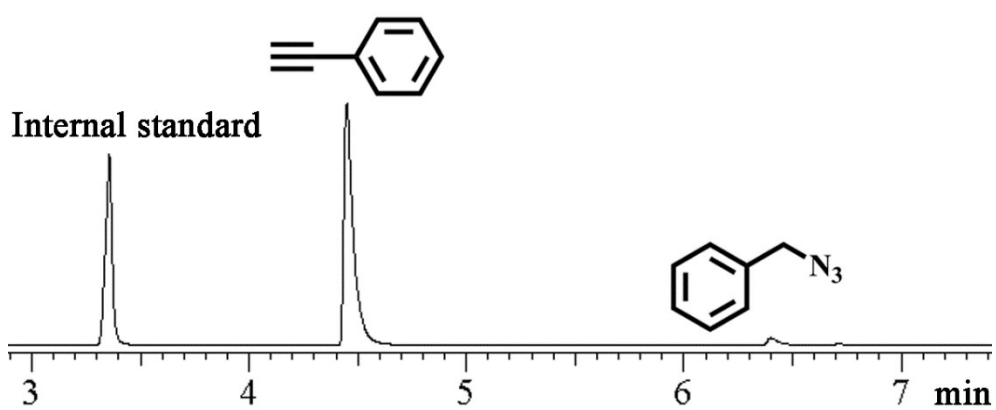
Fig. S14 GC of AAC reactions between benzyl azide and phenylacetylene in different

circles. (a) The first circle, (b) the second circle, (c) the third circle and (d) the fourth circle.
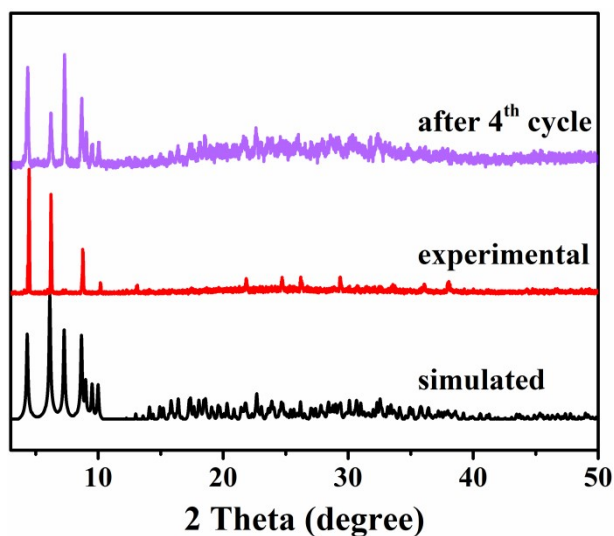
Fig. 15 PXRD patterns of the simulated, the experimental, and four rounds of the AAC reaction catalyzed by **2**.
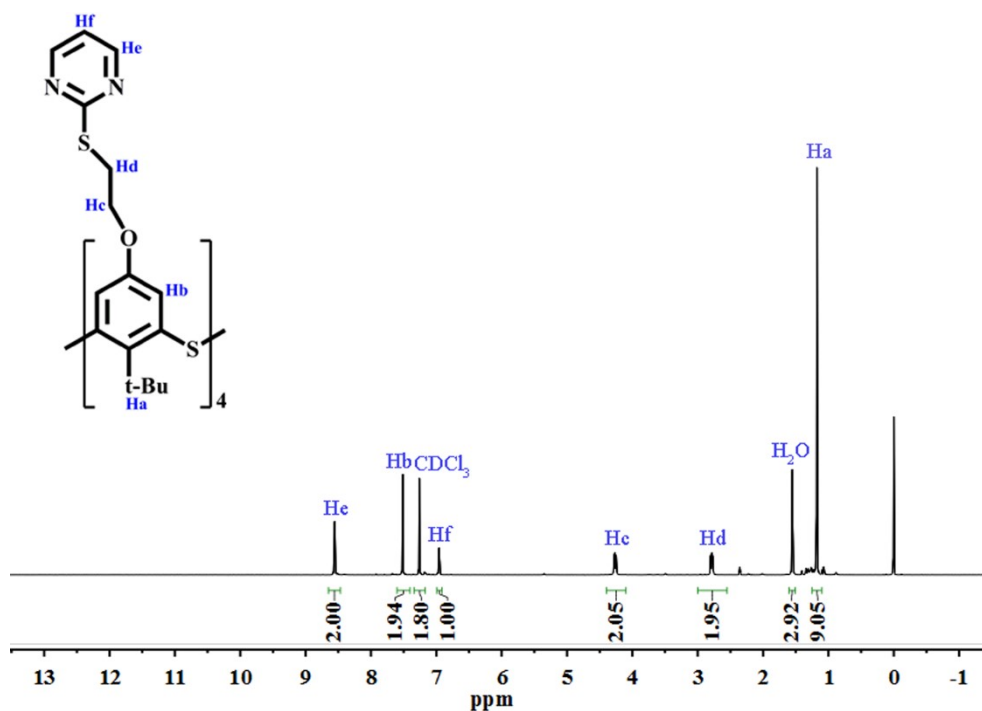
Fig. S16 ^{1}H NMR (500 MHz, CDCl$_3$) for L$_1$, δ 8.54 (dd, 8H), 7.51 (s, 8H), 6.96 (t, 4H), 4.26 (m, 8H), 2.84 (m, 8H), 1.18 (s, 36H).
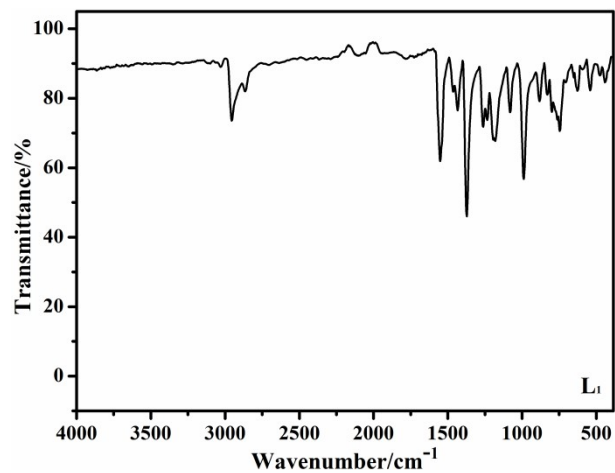
(a)
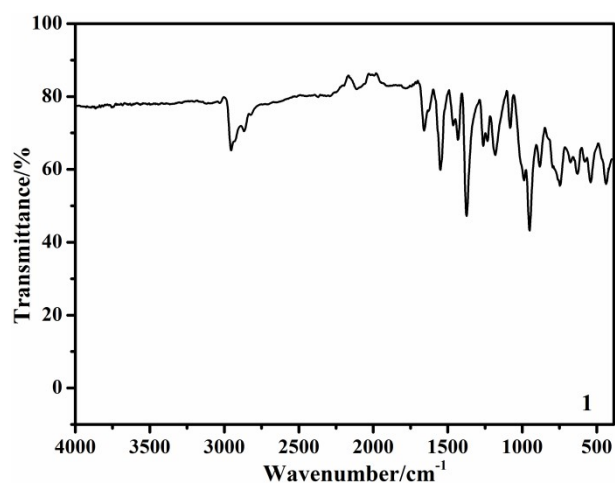
(b)
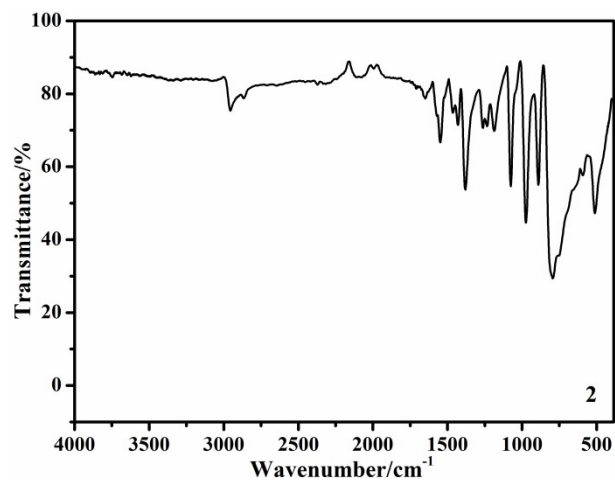
(c)

Fig. S17 IR spectra of (a) L_1, (b) **1** and (c) **2**.
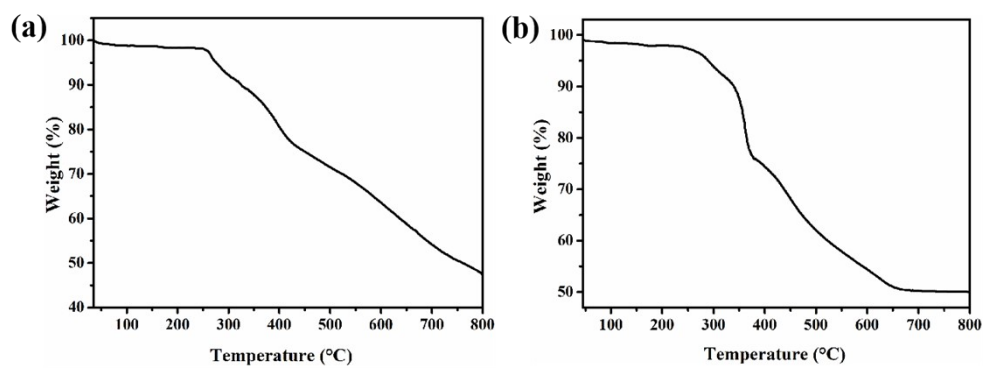
Fig. S18 Thermogravimetric curves. (a) The weight of loss corresponds to the water molecules before 251 °C for **1** (found: 1.82%, calcd: 1.93%). (b) The weight of loss corresponds to the water molecules and EtOH molecules before 241 °C for **2** (found: 2.37%, calcd: 2.41%).
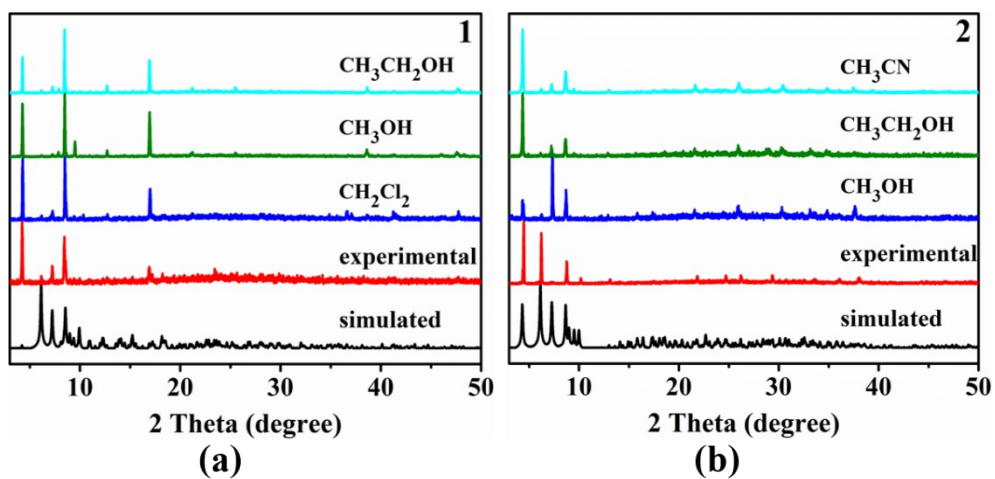
Fig. S19 PXRD patterns of (a) **1** and (b) **2** after immersion in different organic solvents.
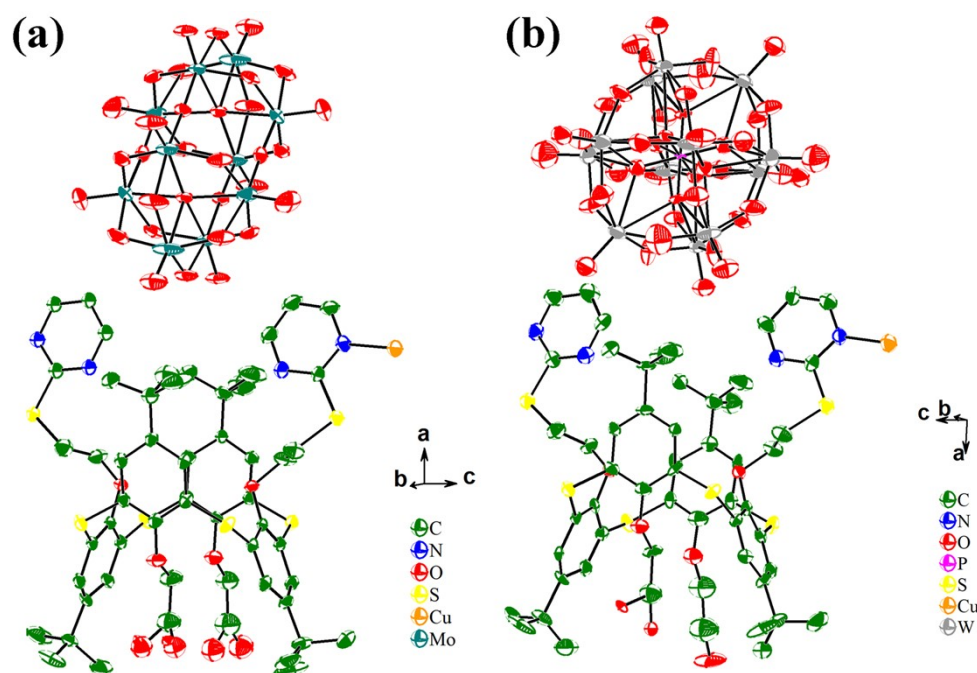
Fig. S20 Diagrams showing anisotropic displacement parameters (ADPs) of (a) **1** and (b) **2**, with the thermal ellipsoids shown at a 30% probability level. All hydrogen atoms are omitted for clarity.

Table S1 Crystallographic data and structural refinements for **1** and **2**.

Complex	1	2
Formula	$C_{56}H_{73}CuN_4O_{24}S_6Mo_5$	$C_{58}H_{76.5}CuN_4O_{28}S_6P_{0.5}W_6$
Mr	1921.78	2652.21
Crystal system	orthorhombic	orthorhombic
Space group	*Pnnm*	*Pnnm*
a (Å)	41.902(4)	40.8437(11)
b (Å)	12.7850(8)	12.7317(7)
c (Å)	15.3738(9)	15.4261(7)
α (°)	90	90
β (°)	90	90
γ (°)	90	90
V (Å^3)	8236.0(10)	8021.7(6)

Z	4	4
D_{calc} (g cm^{-3})	1.550	2.196
F(000)	3856	5012
R_{int}	0.0739	0.0734
GOF on F^2	1.129	1.106
$R1^a$[I >2 σ (I)]	0.1218	0.1138
$wR_2{}^b$(all data)	0.2830	0.2414

$^aR_1 = \Sigma||F_o| - |F_c||/\Sigma|F_o|$. $^bwR_2 = \{\Sigma[w(F_o{}^2-F_c{}^2)^2]/\Sigma w(F_o{}^2)^2]\}^{1/2}$.

Table S2 Selected bond distances (Å) and angles (deg) for Complexes **1** and **2**.

				Complex **1**

Complex 1

N(2)-Cu(1)	1.896(11)	Cu(1)-N(2)$^{\#4}$	1.896(1)
N(2)$^{\#4}$-Cu(1)-N(2)	164.6(9)		

Complex 2

N(1)-Cu(1)	1.877(19)	Cu(1)-N(1)$^{\#4}$	1.877(1)
N(1)-Cu(1)-N(1)$^{\#4}$	165.5(12)		
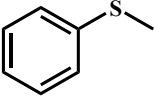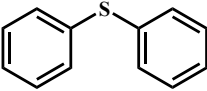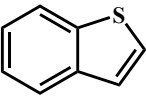
Symmetry code for **1**: $^{\#4}$ *x, y, -z+2*. Symmetry code for **2**: $^{\#4}$ *x, y, -z*.

Table S3 Hydrogen bonds for complexs **1** and **2** (Å and °).

	d(D-H)	d(H···A)	d(D···A)	<(DHA)
C15-H15···O13	0.93	2.423	3.294(2)	155.79(5)
	d(D-H)	d(H···A)	d(D···A)	<(DHA)
C16-H16···O13$^{\#3}$	0.93	2.597	3.196(1)	122.61(3)

Table S4 Catalytic comparison of **1** with related POM-based catalysts.

Substrate	Catalyst	Temp(°C)	Time(h)	Oxidant	Conv.(%)	Ref

(structure: thioanisole, phenyl methyl sulfide)	[a][Zn$_{1.5}$(L$_2$OH)$_3$] · (PMo$_{12}$O$_{40}$) · CH$_3$OH · 2H$_2$O	50	3	TBHP	99	6
	[b](Hbim)$_2$[{Cu(bim)$_2$(H$_2$O)$_2$}$_2${Co$_2$Mo$_{10}$H$_4$O$_{38}$}] · 5H$_2$O	40	4	TBHP	98.4	7
	[c][Co$_2$(L$_3$)$_{0.5}$V$_4$O$_{12}$]·3DMF·5H$_2$O	50	4	TBHP	99	8
	[d][Ag$_4$(PMo$_{12}$O$_{40}$)(L$_4$)$_2$]·OH	40	4	TBHP	99	9
	1	25	3	TBHP	>99	This work
(structure: diphenyl sulfide)	[e][Ag$_3$L$_5$(PMo$_{12}$O$_{40}$)]	50	3	TBHP	91	10
	[a][Zn$_{1.5}$(L$_2$OH)$_3$] · (PMo$_{12}$O$_{40}$) · CH$_3$OH · 2H$_2$O	50	3	TBHP	99	6
	[f](en)[Cu$_3$(ptz)$_4$(H$_2$O)$_4$][Co$_2$Mo$_{10}$H$_4$O$_{38}$] · 24H$_2$O	40	12	TBHP	60.5	7
	1	25	3	TBHP	99	This work
(structure: benzothiophene)	[d][Ag$_4$(PMo$_{12}$O$_{40}$)(L$_4$)$_2$]·OH	40	12	TBHP	4	9
	1	25	12	TBHP	20	This work

[a]L$_2$ = 2,6-bis(2'-pyridyl)-4-hydroxypyridine; [b]bim = benzimidazole; [c]L$_3$ = 2-(2-pyridyl)imidazole functionalized resorcin[4]arene; [d]L$_4$ = tetra[2-(ethylthio)-1-methyl-1H-imidazole]-thiacalix[4]arene; [e]L$_5$ = tetra-[5-(mercapto)-1-methyltetrazole]-thiacalix[4]arene; [f]en = ethylenediamine; ptz = 5-(4-pyridyl)-1H-tetrazole.

References

1 G. M. Sheldrick, *SHELXS-2018, Program for the crystal structure solution*; University of Göttingen: Göttingen, Germany, 2018.

2 L. J. Farrugia, *WINGX: A Windows Program for Crystal Structure Analysis*; University of Glasgow: Glasgow, UK, 1988.

3 G. M. Sheldrick, SHELXL-2018, *Program for the crystal structure refinement*; University of Göttingen: Göttingen, Germany, 2018.

4 N. Kon, N. Iki and S. Miyano, *Tetrahedron Lett.*, 2002, **43**, 2231-2234.

5 A. S. Ovsyannikov, M. H. Noamane, R. Abidi, S. Ferlay, S. E. Solovieva, I. S. Antipin, A. I. Konovalov, N. Kyritsakas and M. W. Hosseini, *CrystEngComm*, 2016, **18**, 691-703.

6 Y.-Q. Zhao, Y.-Y. Liu and J.-F. Ma, *Cryst. Growth Des.*, 2020, **21**, 1019-1027.

7 H. An, Y. Hou, L. Wang, Y. Zhang, W. Yang and S. Chang, *Inorg. Chem.*, 2017, **56**, 11619-11632.

8 M. Craven, D. Xiao, C. Kunstmann-Olsen, E. F. Kozhevnikova, F. Blanc, A. Steiner and I. V. Kozhevnikov, *Appl. Catal. B*, 2018, **231**, 82-91.

9 M.-Y. Yu, T.-T. Guo, X.-C. Shi, J. Yang, X. Xu, J.-F. Ma and Z.-T. Yu, *Inorg. Chem.*, 2019, **58**, 11010-11019.

10 J. Li, P. Du, Y.-Y. Liu and J.-F. Ma, *Dalton Trans.*, 2021, **50**, 1349-1356.